Title

CP49 and filensin intermediate filaments are essential for formation of cold cataract.

Authors

Li, Yuxing

Liu, Xi

Xia, Chun-Hong

et al.

Publication Date

2020

Molecular Vision 2020; 26:603-612 <http://www.molvis.org/molvis/v26/603>
Received 29 January 2020 | Accepted 21 August 2020 | Published 23 August 2020

CP49 and filensin intermediate filaments are essential for formation of cold cataract

Yuxing Li,[1,2] Xi Liu,[2] Chun-hong Xia,[1] Paul G. FitzGerald,[3] Rachel Li,[1] Jessica Wang,[1] Xiaohua Gong[1,2]

[1]Vision Science and Optometry, University of California, Berkeley, Berkeley, CA; [2]Tsinghua-Berkeley Shenzhen Institute (TBSI), UC Berkeley, Berkeley, CA; [3]Department of Cell Biology and Human Anatomy, School of Medicine, University of California, Davis, CA

Purpose: To investigate the molecular and cellular mechanisms of cataract induced by cold temperatures in young lenses of wild-type C57BL/6J (B6), wild-type 129SvJae (129), and filensin knockout (KO) mice. To determine how lens intermediate filament proteins, filensin (BFSP1) and CP49 (BFSP2), are involved in the formation of cold cataract.
Methods: The formation of cold cataract was examined in enucleated lenses at different temperatures and was imaged under a dissecting microscope. Lens vibratome sections were prepared, immunostained with different antibodies and fluorescent probes, and then imaged with a laser confocal microscope to evaluate the protein distribution and the membrane and cytoskeleton structures in the lens fibers.
Results: Postnatal day 14 (P14) wild-type B6 lenses showed cataracts dependent on cold temperatures in interior fibers about 420–875 µm (zone III) and 245–875 µm (zone II and zone III) from the lens surface, under 25 °C and 4 °C, respectively. In contrast, wild-type 129 (with *CP49* gene deletion) and filensin KO (on the B6 background) lenses did not have cold cataracts at 25 °C but displayed a reduced cold cataract, especially in zone III, at 4 °C. Immunofluorescent staining data revealed that CP49 and filensin proteins were uniformly distributed in fiber cell cytosols without cold cataracts but accumulated or aggregated in the cell boundaries of the fibers where cold cataracts appeared.
Conclusions: CP49 and filensin are important components for the formation of cold cataract in young B6 mouse lenses. Accumulated or aggregated CP49 and filensin beaded intermediate filaments in fiber cell boundaries might directly or indirectly contribute to the light scattering of cold cataract. Cold cataract in zone II is independent of beaded intermediate filaments. CP49 and filensin intermediate filaments and other lens proteins probably form distinct high molecular organizations to regulate lens transparency in interior fibers.

Cataract, named for ocular lens opacity, remains the major cause of blindness worldwide [1]. Cold cataract, occurring in the young lenses of various species, including rodents, fishes, cows, and humans, by low temperature, is a reversible opacity in a transparent lens that has been studied to understand the molecular mechanisms associated with lens transparency and light scattering [2,3]. Cold cataract is also an age-dependent phenomenon in mammalian lenses and is thought to result from the aggregation and phase separation of γ-crystallin proteins at low temperatures in vitro and in vivo [2,4,5]. Several studies have further suggested that cold cataracts are associated with change in the supermolecular organization of particular proteins in the lens [6,7]. However, the components of the supermolecular structure leading to the formation of cold cataract are not fully characterized. The physicochemical nature of light scattering elements in lens fibers remains not well understood in the formation of cold cataract.

Correspondence to: Xiaohua Gong, 693 Minor Hall, University of California, Berkeley Berkeley, CA 94720-2020; Phone: (510) 642-2491; FAX: (510) 642-5086; email: xgong@berkeley.edu

Lens-specific beaded intermediate filaments, assembled through the dimerization of CP49 (phakinin or BFSP2) and filensin (BFSP1), are important for fiber cell shape and the stiffness, integrity, and clarity of the lens [8-10]. Previous studies have reported that wild-type 129 mouse substrains, including 129SvJ and 129SvJae (or 129S4), and the wild-type FVB/M mouse strain all contain a deletion in the CP49 (Bfsp2) locus to abolish the lens beaded intermediate filaments [11-13]. Loss of either CP49 or filensin abolishes beaded intermediate filaments and alters interior fiber cell shapes in mouse lenses [14-16]. Beaded intermediate filament proteins have never been suggested to be involved in the formation of cold cataract.

In this study, we characterized the formation of cold cataract in the lenses of young wild-type C57BL/6J (B6), wild-type 129SvJae (129), and filensin knockout (KO) mice with the B6 strain background. The results revealed altered and reduced formation of cold cataract in the CP49 and filensin mutant lenses. Beaded intermediate filaments consisting of CP49 and filensin proteins are likely to be part of the supermolecular structure that is responsible for the reversible formation of cold cataract in the lens core.

METHODS

Mice and formation of cold cataract: Mouse care and breeding were performed according to the Animal Care and Use Committee approved animal protocol (University of California Berkeley, Berkeley, CA) and the ARVO Statement for the Use of Animals in Ophthalmic and Vision Research. Three mouse strains, C57BL/ 6J wild-type, 129 wild-type [12], and filensin gene knockout [15] on the C57BL/6J background, were used. Enucleated eyeballs were immediately collected from mice euthanized by CO_2 inhalation and were dissected in 4 °C cold PBS (137 mM NaCl, 2.7 mM KCl, 10 mM Na_2HPO_4, 1.8 mM KH_2PO_4, pH 7.4) to prepare the 4 °C treated lens samples or in PBS at room temperature to prepare the 25 °C and 37 °C treated lens samples. The dissected lenses were immediately transferred into fresh PBS at 4 °C, 25 °C, and 37 °C, respectively, for imaging under a Leica MZ16 (Leica, Wetzlar, Germany) dissecting microscope with a digital camera. The whole procedure including dissecting and imaging took about 10–15 min. A transparent lens developed a full cold cataract within less than 3 min after immersion in 4 °C PBS, and a cold cataract disappeared within less than 3 min after immersion in 37 °C PBS. We also made a small-interval temperature controller to sequentially change temperatures from 4 °C to 25 °C by using the thermoelectric cooler Peltier 12V CL-C067 (Heke Tech, Shenzhen, China) with a plate (40 × 40 × 3.87 mm) equipped with copper tubes for the circulating solution and a fan to dissipate heat in air. This temperature controller utilizes a feedback signal that forms a closed-loop control refrigeration system to detect, change, or maintain the temperature of the PBS in the plate.

Statistical analysis: Statistical significance was determined with one-way analysis of variance (ANOVA) with Tukey's post-hoc test, using GraphPad Prism software (San Diego, CA). P values less than or equal to 0.01, 0.001, and 0.0001 were considered statistically significant.

Lens vibratome section and immunohistochemistry: For the examination of 4 °C induced cold cataract, fresh lenses were dissected in 4 °C PBS and fixed in 4% paraformaldehyde/PBS solution at 4 °C for overnight. For the 25 °C or 37 °C treated lens samples, fresh lenses were dissected in PBS at room temperature and then transferred into 25 °C or 37 °C 4% paraformaldehyde/PBS solution for 3–5 h fixation. Fixed lenses were washed with PBS three times before being embedded in 4% low-melting agarose gel and then were superglued to an aluminum mounting block as in the following procedures: A drop of 4% low melted agarose (about 35 µl) was added on the surface of the aluminum mounting block. A wedge was cut in the solidified agarose gel to hold a lens, which was oriented for cutting either anterior-posterior (A/P; along the optical axis) or cross-sectional (along the lens equator) planes. Then 0.4 µl of superglue was added to the wedge (not attached to the lens) to glue the agarose gel with the oriented lens on the aluminum mounting block. The entire lens was further covered with agarose. After the agarose gel solidified, the block with the agarose embedded lens was mounted on a Leica VT1000 S Vibratome, and lens sections with 100 µm thickness were cut. Lens sections around the lens equator were collected for immunostaining. The lens vibratome sections were first incubated with a blocking solution containing 3% wt/vol bovine serum albumin (BSA; Gemini Bio-products, West Sacramento, CA), 3% vol/vol normal goat serum (Vector Laboratories, Inc., Burlingame, CA), and 0.3% vol/vol Triton X-100 (Sigma-Aldrich, St. Louis, MO) in PBS for 2 h, followed by incubation with rabbit polyclonal antibodies against CP49 or filensin (generated in Paul Fitzgerald's laboratory at the University of California at Davis) at 4 °C for overnight. After washing three times in PBS, the sections were incubated in rhodamine-labeled secondary antibodies and fluorescein (FITC)-phalloidin (Vector Laboratories, Inc.) for 2 h at room temperature. Then the lens sections were washed three times in PBS and were mounted in Vectashield mounting medium with 4',6-diamidino-2-phenylindole (DAPI; Vector Laboratories). Fluorescent images were collected using a Zeiss LSM 700 confocal microscope. ImageJ software was used to quantify the intensity and distribution of the immunostained CP49 and filensin protein signals in different areas in regions in lens zones I, II, and III. The signal intensity ratios between the cellular boundary and cytosol were analyzed in selected areas in the three zones. Immunostaining analysis for each antibody was performed in lens vibratome sections from at least three different mice including female and male mice for each genotype.

Immunostaining of single lens fiber cells: Fixed lenses with capsule were cracked open from the lens center along the A/P axis to produce three or four pieces of lens mass by using forceps with a fine sharp tip (Student Dumont #5 Forceps, Fine Science Tools, Foster City, CA). The lens pieces were fixed in a drop of 4% paraformaldehyde/PBS solution for 5 min and then washed with PBS drops three times under the dissecting microscope. Lens pieces from the lens cortex to the lens core were used for whole mount staining with rabbit polyclonal anti-filensin antibody on parafilm paper in a small humidified chamber. The same immunostaining procedure for the lens vibratome sections was used. To maximize the dissociation of single lens fibers, fine forceps were used to tease apart the lens pieces into small bundles before they were mounted in Vectashield mounting medium with DAPI. Low-magnification images of whole mount lens pieces were used to determine the location of single fibers from the lens

surface, and high-magnification images of single fibers that partly detached from the surface of bundled fibers in different zones were collected under a Zeiss LSM 700 confocal microscope. Filensin protein staining images of single fibers in representative regions of zones I, II, and III were analyzed for the intensity plot of the single fiber cell surface by using ImageJ software.

RESULTS

Differences in formation of cold cataract in B6 wild-type, 129 wild-type, and B6 filensin KO mouse lenses: We examined transparency or opacity in enucleated fresh lenses from P14 B6 wild-type (B6WT), 129 wild-type (129WT), and B6 filensin KO mice at three representative temperatures, 37 °C, 25 °C, and 4 °C (Figure 1). The B6WT lenses, immersed in cold PBS in vitro, showed typical cold cataracts, as opacity occurred in the lens nucleus at 25 °C, and larger opacity that expanded toward the cortex appeared at 4 °C, while the lens periphery remained clear (Figure 1A). Unexpectedly, the 129WT and B6 filensin KO lenses had no opacity at 25 °C but showed similar opacity with reduced light scattering in the lens core at 4 °C (Figure 1B,C). More than three male and three female 129WT and B6 filensin KO mice were examined, and we observed the identical cold cataract phenomenon. There were no noticeable differences in the formation of cold cataract among lenses from more than three different male and female mice. No phenotypic difference was observed between the two lenses of a single mouse from these mouse lines.

Quantitative densitometry scanning measurements of these lens images at the equatorial plane further revealed that the light scattering distribution of the B6WT cold cataract (Figure 1D) obviously differed from those of the 129WT and B6 filensin KO cold cataracts which showed gradually reduced opacity toward the lens core at 4 °C (Figure 1E,F). The size of the P14 lenses of different mice was similar with a diameter about 1,735 ± 50.00 µm (n = 9). The diameters of the 4 °C cold cataracts were 1,279 ± 25.00 µm for B6WT, 1,264 ± 21.00 µm for 129WT, and 1,276 ± 26.00 µm for B6 filensin KO, about 73% of the whole lens diameter. However, the diameter of the 25 °C cold cataracts in the B6WT mice, 939 ± 27.0 µm, was about 27% smaller than that of the 4 °C cold cataracts (Figure 1G).

The formation of cold cataracts was completely reversible in all mouse lenses. Lens opacity disappeared within minutes when the cold cataractous lenses were immersed in the 37 °C PBS solution. We further assessed the recovery of P14 B6WT and B6 filensin KO lens transparency during a continuous warm-up course from 4 °C to 25 °C in PBS and then 37 °C (Appendix 1).

Based on the diameters of the cold cataracts at 4 °C and 25 °C, we proposed a schematic cold cataract model by arbitrarily dividing the lens into three zones (I, II, and III). Zone I represents the transparent part of the lens cortex that never develops cold cataracts, zone II covers the expanded area of the cold cataract at 4 °C, and zone III covers the lens core region where 25 °C induced cold cataract occurs. The B6WT cold cataract seemed to be more opaque than the 129WT and B6 filensin KO cold cataracts. The 129WT mouse strain is known to contain a *CP49* gene deletion. The results suggested that CP49 and filensin are important for the formation of cold cataracts. To understand the roles of CP49 and filensin in the formation of cold cataracts, we performed immunostaining to determine the distributions of the CP49 and filensin proteins in selective areas of zones I, II, and III in lenses treated with different temperatures.

Formation of cold cataract correlates with accumulations of CP49 and filensin proteins in interior fiber cell boundaries: Lens intermediate filaments composed by CP49 and filensin play essential roles in maintaining the cell shape of the lens fiber and regulating cell morphogenesis in the maturation of fiber cells. We characterized the distribution of the CP49 and filensin proteins in the inner fibers of the B6WT lenses (zone I to zone III) under the treatment of different temperatures. Confocal images of the lens cross-sectional view revealed CP49 immunostaining in lens fibers from the periphery to the core. Uniform CP49 signals appeared in the zone I, II, and III lens fibers in the 37 °C treated samples as well as in zone I fibers of the 25 °C and 4 °C treated lens samples (Figure 2). However, evenly segregated CP49 signals appeared in zone II interior fibers, but unevenly segregated CP49 signals occurred in the zone III fibers of the lens core in the 25 °C treated samples. Moreover, irregularly aggregated or accumulated CP49 signals often appeared along the fiber cell boundaries in the zone II and zone III fibers of the 4 °C treated lens samples (Figure 2A–D). Quantitative measurements of the CP49 signal intensity ratios between the fiber cell boundaries versus the cytosol in zones I, II, and III of these samples are shown in Table 1. These data suggest that increased CP49 accumulative signals near fiber cell boundaries were statistically significant in zone II and zone III of the 4 °C treated lens samples and in zone III of the 25 °C treated lens samples, which were correlated with the appearance of cold cataracts (Figure 2E–G).

Immunohistochemical analysis was performed to examine the filensin distributions in B6WT lens vibratome sections along the anterior-posterior axis. Similar to the CP49

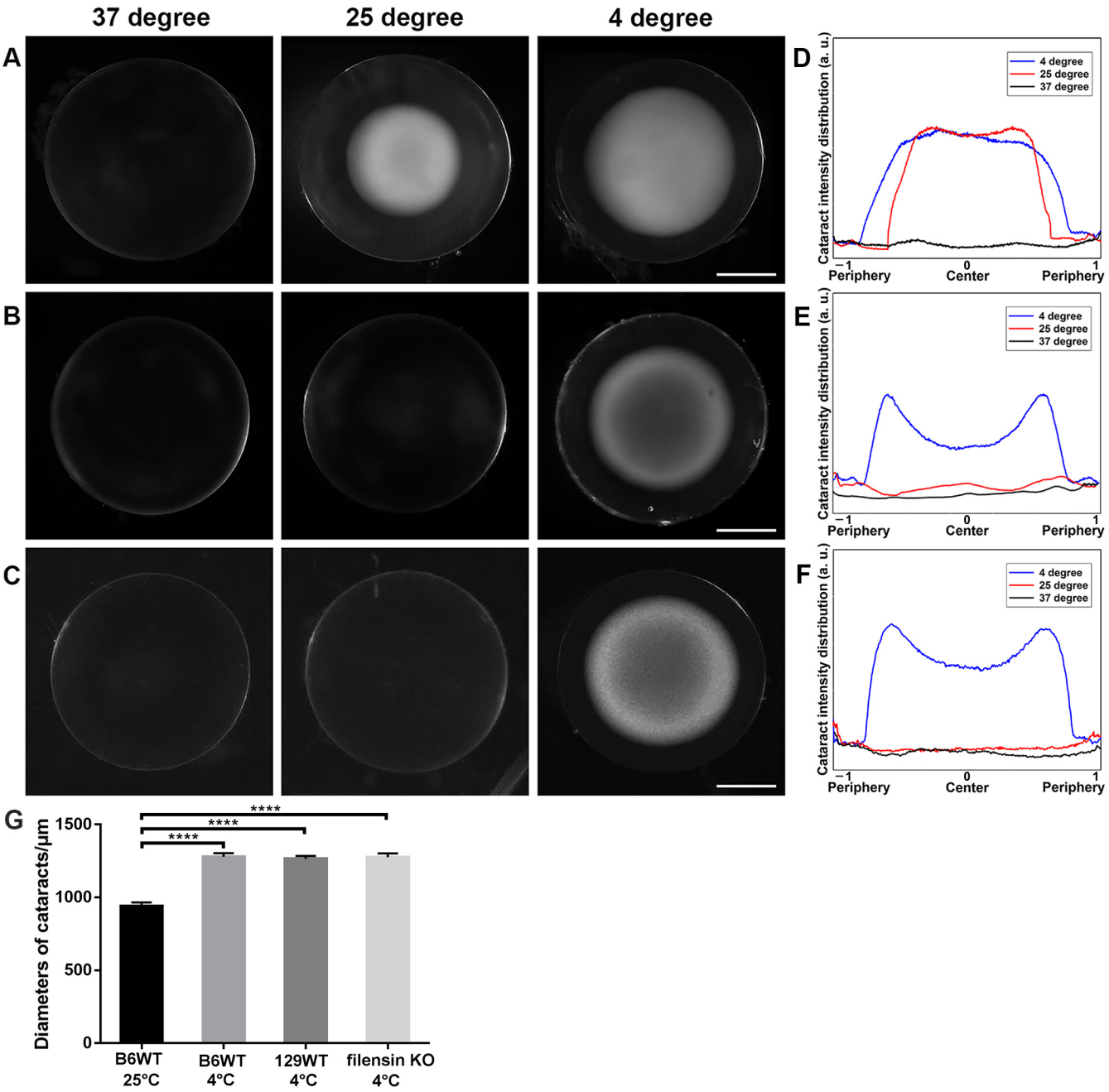

Figure 1. Formation of cold cataract in lenses of P14 mice. Representative anterior-view images of B6 wild-type (B6WT, **A**), 129 wild-type (129WT, **B**), and B6 filensin knockout (filensin KO, **C**) lenses at 37 °C, 25 °C, and 4 °C. Cataracts (white opacity in the lens) appeared in the 25 °C and 4 °C treated B6WT lenses but only in the 4 °C treated 129WT lens and 4 °C treated B6 filensin KO lens. These lens images were quantitatively measured with ImageJ with line scanning for cataract intensity (y-axis) versus the lens middle plane (x-axis) from the left surface (−1 on the graphs) to the right surface (+1 on the graphs). The lens center is marked as 0; the blue line is for 4 °C, the red line for 25 °C, and the black line for 37 °C in the B6WT (**D**), 129WT (**E**), and B6 filensin KO (**F**) lenses. Bar graphs show a statistic comparison of the diameters of the cold cataracts (**G**). The 25 °C induced cold cataract is statistically significantly smaller than all 4 °C induced cold cataracts (n = 4, ****p≤0.0001). Scale bar for **A**–**C**, 0.5 µm. Statistical significance was determined with one-way analysis of variance (ANOVA) with Tukey's post-hoc test. **p≤0.01, ***p≤0.001, ****p≤0.0001.

protein distributions, the filensin signals were uniformly distributed in all fibers of the 37 °C treated lens samples but became unevenly accumulated near the fiber cell boundaries in zone III of the 25 °C treated lens samples, as well as in the

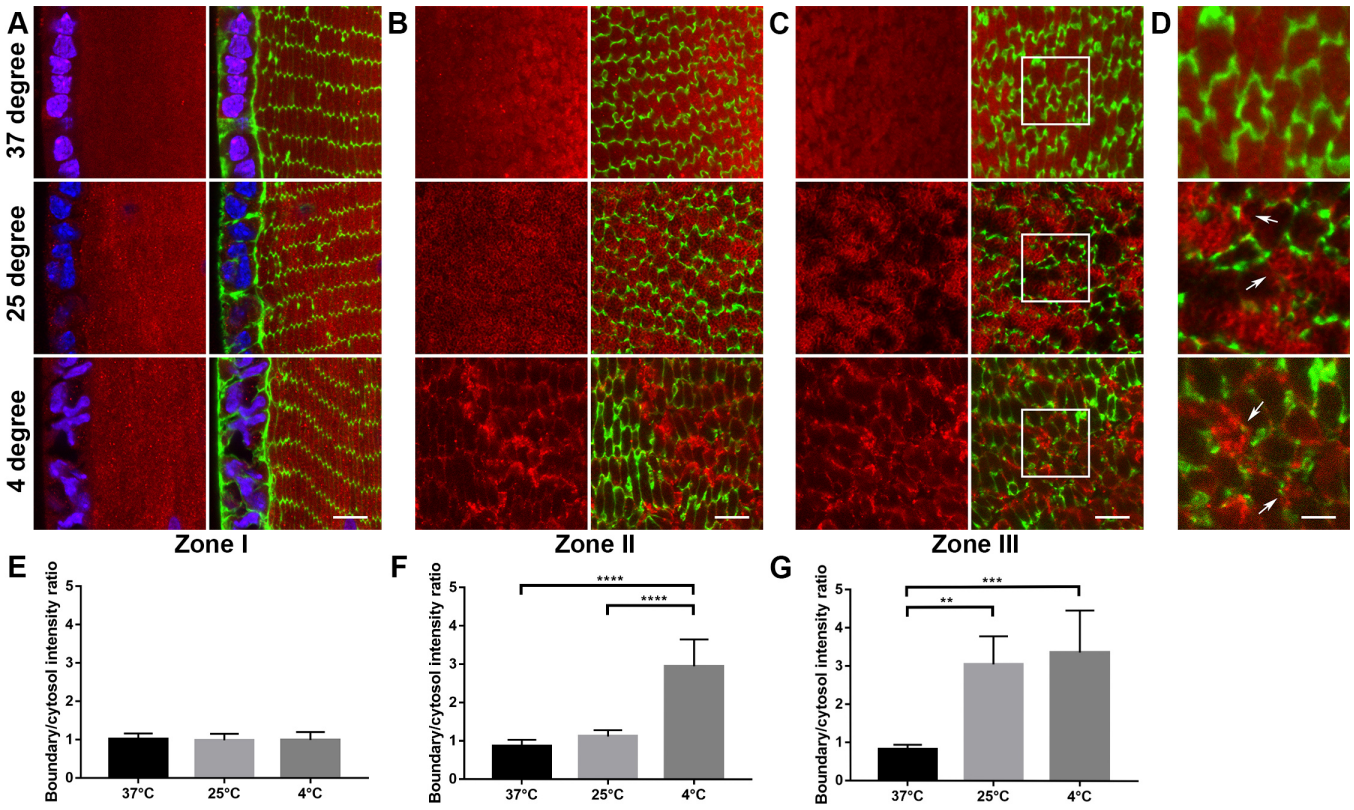

Figure 2. Confocal fluorescent images show CP49 protein distribution in lens fibers at zone I, zone II, and zone III from the 37 °C, 25 °C, and 4 °C treated B6WT lenses. The lens cross-sectional samples were immunolabeled with anti-CP49 antibody (red), fluorescein (FITC)-phalloidin (green), and 4',6-diamidino-2-phenylindole (DAPI; blue). The left panels are CP49 alone, and the right panels are merged with F-actin and nuclei. **A**, **B**, and **C** represent an area (50 µm × 50 µm) of fibers located in 0–50, 325–375, and 425–475 µm from the lens equatorial surface, respectively (see the locations of zones I, II, and III in **A**, **B**, and **C**, respectively, illustrated in Figure 5). **D**: Enlarged images of the white-box regions in zone III (**C**); white arrows indicate CP49 accumulation. **E**, **F**, and **G**: Bar graphs show CP49 staining intensity ratios between fiber cell boundaries versus the cytosol in zones I, II, and III that were quantitatively measured and compared as mean ± standard deviation (SD; n = 3, per sample group). **E**: Among three different temperatures, there was no statistically significant difference in the CP49 distribution in zone I. **F**: However, the CP49 boundary/cytosolic intensity ratio in the 4 °C treated fibers was statistically significantly higher than those in the 37 °C and 25 °C treated fibers in zone II (***p≤0.001), and the 4 °C and 25 °C treated fibers showed statistically significantly higher CP49 ratios than the 37 °C treated fibers in zone III (**G**, **p≤0.01 or ***p≤0.001). Scale bar: **A**–**C**, 10 µm; **D**, 4 µm.

zone II and zone III fibers of the 4 °C treated lens samples (Figure 3A–D). Quantitative measurements of the filensin signal intensity ratios between the fiber cell boundaries versus the cytosol in zones I, II, and III of these samples are shown in Table 2. These data suggest that the accumulated filensin signals near the fiber cell boundaries were statistically significant in zone II and zone III of the 4 °C treated lens samples and in zone III of the 25 °C treated lens samples, which were correlated with the appearance of cold cataracts (Figure 3E–G). Thus, the results suggest that uneven accumulations of lens beaded filaments, consisting of CP49 and filensin proteins near fiber cell boundaries, were correlated with the formation of cold cataract in lens inner fibers in zone II and zone III.

Table 1. CP49 signal intensity ratios between fiber cell boundaries and cytosols (n=3)

Temperature	37 °C	25 °C	4 °C
Zone I	1.01±0.15	0.98±0.17	0.99±0.2
Zone II	0.86±0.17	1.12±0.15	2.94±0.7
Zone III	0.82±0.11	3.04±0.73	3.35±1.09

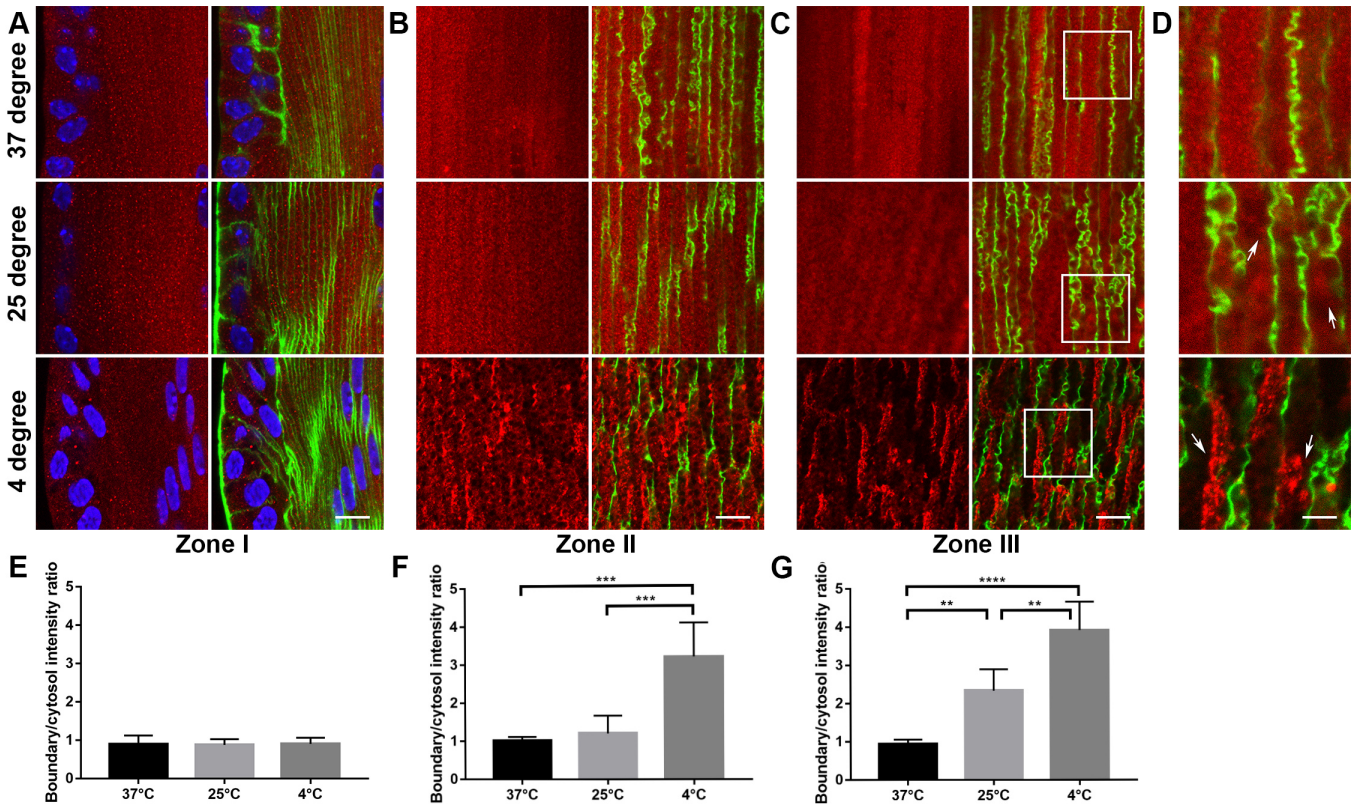

Figure 3. Confocal fluorescent images show filensin protein distribution in lens fibers at zone I, zone II, and zone III from the 37 °C, 25 °C, and 4 °C treated B6WT lenses. The lens A/P sectional samples were immunolabeled with anti-filensin antibody (red), fluorescein (FITC)-phalloidin (green), and 4',6-diamidino-2-phenylindole (DAPI; blue). The left panels are filensin alone, and the right panels are merged with F-actin and nuclei. **A**, **B**, and **C** represent an area (50 µm × 50 µm) of fibers located in 0–50, 325–375, and 425–475 µm from the lens equatorial surface, respectively (see the locations of zones I, II, and III in **A**, **B**, and **C**, respectively, illustrated in Figure 5). **D**: Enlarged images of the white-box regions in zone III (**C**); white arrows indicate filensin accumulation. **E**, **F**, and **G**: Bar graphs show that filensin staining intensity ratios between fiber cell boundaries versus the cytosol in zones I, II, and III were quantitatively measured and compared as mean ± standard deviation (SD; n = 3, per sample group). **E**: Among three different temperatures, the distribution of CP49 showed no statistically significant difference in zone I. However, the CP49 boundary/cytosolic intensity ratio in the 4 °C treated fibers was statistically significantly higher than those in the 37 °C and 25 °C treated fibers in zone II (**F**, ***p≤0.001), and the comparisons among the 4 °C, 25 °C, and 37 °C treated fibers in zone III showed statistically significant differences (**G**, **p≤0.01, ****p≤0.0001). Scale bar: **A**–**C**, 10 µm; **D**, 4 µm.

We also performed immunohistochemical analysis of filensin and CP49 in the 129WT lens vibratome sections. The confocal fluorescent images showed extremely low levels of the filensin protein in lens fibers at zones I, II, and III from the 37 °C, 25 °C, and 4 °C treated samples (Appendix 2) and the absence of the CP49 protein or background signal in all lens fibers (Appendix 3). Therefore, the cold cataracts in the 129WT lenses were independent of the beaded intermediate filaments in the interior lens fibers.

Uneven accumulations of filensin proteins detected in interior single fibers of cold cataract lens: To further characterize the changes in filensin protein distributions in cold temperature–induced cataractous lens, we performed double-labeling of anti-filensin antibody and FITC-phalloidin (F-actin) in single

Table 2. Filensin signal intensity ratios between fiber cell boundaries and cytosols (n=3)

Temperature	37 °C	25 °C	4 °C
Zone I	0.9±0.22	0.88±0.15	0.9±0.16
Zone II	1.01±0.1	1.2±0.46	3.2±0.89
Zone III	0.93±0.11	2.33±0.56	3.92±0.74

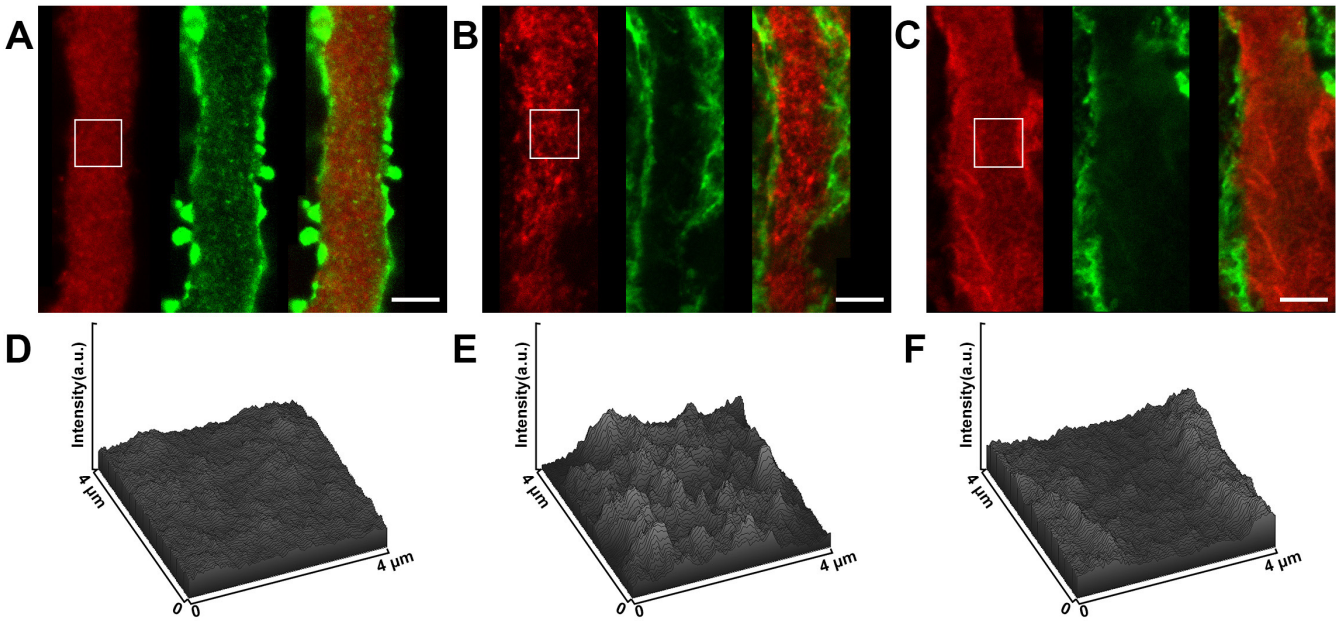

Figure 4. Representative confocal images of filensin distributions on the long sides of hexagonal single fibers were collected from zone I, zone II, and zone III of lens pieces double-labeled with anti-filensin antibody (red) and fluorescein (FITC)-phalloidin (green). **D**, **E**, and **F** filensin signal intensity in white-box regions in images (**A**, **B**, and **C**) were scanned, and the fibers of zone II and zone III displayed uneven patterns. Scale bar: 4 μm.

lens fiber cells at different zones of the 4 °C treated B6WT lens. Filensin staining signals were uniformly distributed in the single lens fiber cells of zone I (Figure 4A), unevenly distributed in the single lens fiber cells of zone II (Figure 4B), and predominately accumulated near fiber cell boundaries in single lens fiber cells of zone III (Figure 4C). Quantitative analysis further verified that uneven accumulations of filensin proteins were correlated with the formation of cold cataracts in zone II (Figure 4E) and zone III (Figure 4F). These single lens fiber cell results, consistent with the B6WT lens vibratome section data, revealed that beaded intermediate filaments are important in the formation of cold cataracts.

DISCUSSION

This study demonstrated that zone I remained transparent, zone II became opaque only at 4 °C in P14 B6WT lenses, while zone III became opaque at 25 °C but remained transparent in 129WT and B6 filensin KO lenses. Based on these results, a schematic lens model is proposed for the formation of cold cataract (Figure 5A). The 129WT mice contain a CP49 gene deletion and resemble the lens phenotypes of CP49 knockout mice [12]. CP49 and filensin proteins coassemble into lens-specific beaded intermediate filaments as one of the major cytoskeletal structures in lens fibers [10,11,15]. Obvious differences in the formation of cold cataracts between the B6WT lens and the 129WT or B6 filensin KO lenses suggest that beaded intermediate filament dependent and independent events contribute to the formation of cold cataracts, and beaded intermediate filaments are essential for the formation of cold cataracts in the lens core (zone III).

Immunostaining data revealed that temperature changes could affect the distribution or aggregation of filensin and CP49 in lens interior fibers. A sketch model showed even distribution of filensin and CP49 proteins in an interior fiber at 37 °C but enriched accumulation or aggregation of filensin and CP49 proteins near fiber cell boundaries at 4 °C (Figure 5B). This work supported the concept that the supermolecular organization of protein complexes rather than a single protein is the cause of the formation of cold cataracts and that different protein complexes associated with various posttranslational modifications may be involved in cataract variances between zone II and zone III. This is supported by several previous studies in fish, duck, rat, flounder, and bovine lenses [3,7,17]. This work showed for the first time that beaded intermediate filaments composed by CP49 and filensin are essential components of the supermolecular organization in the lens core. Moreover, there must be another protein complex that is responsible for cold cataracts in zone II of 129WT and B6 filensin KO lenses.

Substantial accumulations of CP49 and filensin filaments in fiber cells under low temperatures might increase light scattering to lead to the formation of cold cataract, suggesting the involvement of cytoskeleton and other related proteins such as alpha-crystallin. Several proteins, including aquaporin 0 and periplakin, have been reported to be potential linkers between intermediate filaments and plasma membrane or cytoskeleton structures [18-21]. The distribution of lens intermediate filament proteins filensin and CP49 is highly regulated in different regions of inner fiber cells [10,22]; post-translational modifications of filensin and CP49 proteins also occur in the transition zone, which is similar to the location in zone II (Figure 5A) of inner fibers [23]. It remains to be investigated whether and how postnatal modifications or phase transition of filensin, CP49, and alpha-crystallins are associated with the cold cataract in zone III. Previous studies suggested that temperature can affect the assembly, disassembly, and aggregation of vimentin intermediate filaments [24,25]. However, vimentin intermediate filaments are used only in the lens periphery where no cold cataract forms. Thus, vimentin is not involved in the formation of cold cataracts in mice. It will be important to determine whether or how CP49 and filensin intermediate filaments undergo temperature-dependent changes in vitro and to identify the membrane protein complexes tethering CP49 and filensin intermediate filaments in interior lens fiber cells in vivo. We also characterized actin filaments in different zones of lenses treated at different temperatures and found no solid evidence to support their involvement in formation of cold cataract.

Several studies reported that the phase separation and aggregation and precipitation of γ-crystallin proteins were the causes of cold cataracts in the lens core in vitro and in vivo [2,26-28]. However, those studies provided only correlative evidence to support the potential involvement of γ-crystallin proteins in the formation of cold cataract in vivo. To date, no γ-crystallin knockout mice have been generated to confirm the essential role of γ-crystallin in the formation of cold cataract in vivo. In a previous study, we reported that a mouse γD-crystallin V76D mutation abolished cold cataracts but developed a severe nuclear cataract, which was associated with substantial pathological changes, including disrupted denucleation, intranuclear protein aggregates, increased lens water-insoluble proteins, and a loss of gap junctions in inner fibers [29]. Therefore, the disappearance of the cold cataract is likely a secondary pathological event in mutant γD V76D lenses. A recent study elegantly revealed that liquid-liquid phase separation of six gamma-crystallin proteins in the Antarctic toothfish depends on their surface positively charged residues (arginine and lysine) for lens protein–protein interactions [30]. No alteration of γ-crystallin proteins has been found in filensin knockout or CP49 knockout lenses [14-16]. There is no evidence to suggest that CP49 and filensin intermediate filaments interact with γ-crystallin. This work indicated that γ-crystallin may not be adequate for the formation of cold cataract.

The formation of cold cataracts in the zone II inner fibers of B6 filensin KO and 129WT lenses is not related to beaded intermediate filaments. A different high molecular

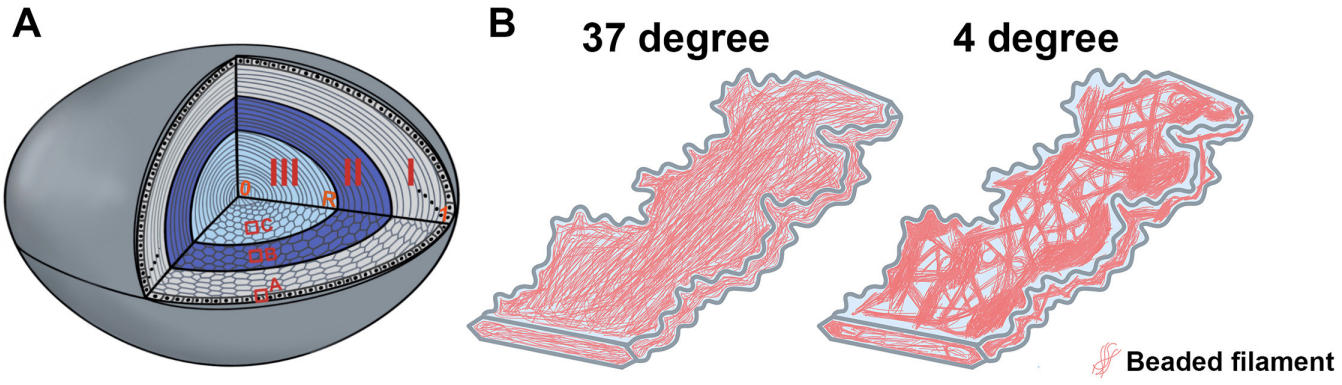

Figure 5. Illustration of lens structures and changes of intermediate filaments in the formation of cold cataract. **A**: A schematic lens model shows three zones (I, II, and III) according to the 25 °C induced cold cataract in zone III and the 4 °C degree induced cold cataract in zone II and zone III in P14 B6 wild-type lenses. The red boxes (**A**, **B**, and **C**) indicate the locations of the lens images in Figure 2, Figure 3, and Figure 4. The radius (R) of the P14 lens from the lens capsule (1) to the lens center (0) is about 875 µm. Zone I fibers (gray) cover 0–245 µm in depth, zone II (dark blue), 245–420 µm in depth, and zone III (light blue), 420–875 µm in depth from the lens surface. **B**: An interior hexagonal fiber cell model shows the change in the CP49 and filensin beaded intermediate filaments from uniform distribution at 37 °C to intermittent accumulation at 4 °C.

organization is likely responsible for cold cataract in zone II. The unique differences in the formation of cold cataracts between the B6WT and 129WT lenses reflect the involvement of multiple distinct high molecular organizations in lens inner fibers during development. Mouse cold cataract remains a fascinating model for understanding the maturation and transparency of fiber cells during lens development at young ages. Future work is necessary to address the molecular mechanism for how CP49 and filensin filaments are accumulated near the fiber cell boundary in the lens at low temperatures.

APPENDIX 1. COLD CATARACT RECOVERY VERIFIED FROM 4 °C TO 37 °C TREATMENTS.

To access the data, click or select the words "Appendix 1." Sequential lens images at different temperatures show a recovery course from a cold cataract in a P14 B6WT lens (A) and a P14 129WT lens (B). Representative lens images at 4 °C, 11 °C. 19 °C and 25 °C were subjected to quantitative measurements by image J scans along the equatorial line (C for B6WT and D for 129WT) from the left surface to the right surface, and the lens diameter was arbitrarily normalized to 2. B6WT lens fully recovered its transparency at 37 °C and 129WT lens became clear at 25 °C.

APPENDIX 2.

To access the data, click or select the words "Appendix 2." Confocal fluorescent images show extremely low levels of filensin proteins in lens fibers at zones I (A), II (B) and III (C) of 37 °C, 25 °C and 4 °C treated 129WT lenses. The lens cross-sectional samples were immunolabeled with anti-filensin antibody (red), FITC-phalloidin (green) and DAPI (blue); the left panels are filensin alone and the right panels are merged with F-actin and nuclei. (D) Enlarged images of the white-boxed areas in zone III in (C). Scale bar: A-C, 10 μm; D, 4 μm.

APPENDIX 3.

To access the data, click or select the words "Appendix 3." Confocal fluorescent images show no CP49 proteins in lens fibers at zones I (A), II (B) and III (C) from 37 °C, 25 °C and 4 °C treated 129WT lenses. The lens cross-sectional samples were immunolabeled with anti-CP49 antibody (red), FITC-phalloidin (green) and DAPI (blue); the left panels are CP49 alone and the right panels are merged with F-actin and nuclei. (D) Enlarged images of the white-boxed regions in zone III (C). Scale bar: A-C, 10 μm; D, 4 μm.

ACKNOWLEDGMENTS

Supported by National Eye Institute Grants, R01EY013849 (X. Gong) and R01EY027430 (PG. FitzGerald) and the research fund from the Tsinghua-Berkeley Shenzhen Institute. Yuxing Li is supported by a research fund of the Tsinghua-Berkeley Shenzhen Institute.

REFERENCES

1. Donaldson PJ, Grey AC, Maceo Heilman B, Lim JC, Vaghefi E. The physiological optics of the lens. Prog Retin Eye Res 2017; 56:e1-24. [PMID: 27639549].
2. Lo WK. Visualization of crystallin droplets associated with cold cataract formation in young intact rat lens. Proc Natl Acad Sci USA 1989; 86:9926-30. [PMID: 2602383].
3. Sivak JG, Stuart DD, Weerheim JA. Optical performance of the bovine lens before and after cold cataract. Appl Opt 1992; 31:3616-20. [PMID: 20725332].
4. Zigman S, Lerman S. A Cold Precipitable Protein in the Lens. Nature 1964; 203:662-3. [PMID: 14250998].
5. Lerman S, Megaw JM, Gardner K, Ashley D, Long RC Jr, Goldstein JH. NMR analyses of the cold cataract. II. Studies on protein solutions. Invest Ophthalmol Vis Sci 1983; 24:99-105. [PMID: 6826319].
6. Banh A, Sivak JG. Laser scanning analysis of cold cataract in young and old bovine lenses. Mol Vis 2004; 10:144-7. [PMID: 15014370].
7. Loewenstein MA, Bettelheim FA. Cold cataract formation in fish lenses. Exp Eye Res 1979; 28:651-63. [PMID: 467522].
8. FitzGerald PG. Lens intermediate filaments. Exp Eye Res 2009; 88:165-72. [PMID: 19071112].
9. Yoon KH, Blankenship T, Shibata B, Fitzgerald PG. Resisting the effects of aging: a function for the fiber cell beaded filament. Invest Ophthalmol Vis Sci 2008; 49:1030-6. [PMID: 18326727].
10. Song S, Landsbury A, Dahm R, Liu Y, Zhang Q, Quinlan RA. Functions of the intermediate filament cytoskeleton in the eye lens. J Clin Invest 2009; 119:1837-48. [PMID: 19587458].
11. Alizadeh A, Clark J, Seeberger T, Hess J, Blankenship T, FitzGerald PG. Characterization of a mutation in the lens-specific CP49 in the 129 strain of mouse. Invest Ophthalmol Vis Sci 2004; 45:884-91. [PMID: 14985306].
12. Sandilands A, Wang X, Hutcheson AM, James J, Prescott AR, Wegener A, Pekny M, Gong X, Quinlan RA. Bfsp2 mutation found in mouse 129 strains causes the loss of CP49′ and induces vimentin-dependent changes in the lens fibre cell cytoskeleton. Exp Eye Res 2004; 78:875-89. [PMID: 15037121].
13. Simirskii VN, Lee RS, Wawrousek EF, Duncan MK. Inbred FVB/N mice are mutant at the cp49/Bfsp2 locus and lack beaded filament proteins in the lens. Invest Ophthalmol Vis Sci 2006; 47:4931-4. [PMID: 17065509].

14. Alizadeh A, Clark JI, Seeberger T, Hess J, Blankenship T, Spicer A, FitzGerald PG. Targeted genomic deletion of the lens-specific intermediate filament protein CP49. Invest Ophthalmol Vis Sci 2002; 43:3722-7. [PMID: 12454043].

15. Alizadeh A, Clark J, Seeberger T, Hess J, Blankenship T, FitzGerald PG. Targeted deletion of the lens fiber cell-specific intermediate filament protein filensin. Invest Ophthalmol Vis Sci 2003; 44:5252-8. [PMID: 14638724].

16. Sandilands A, Prescott AR, Wegener A, Zoltoski RK, Hutcheson AM, Masaki S, Kuszak JR, Quinlan RA. Knockout of the intermediate filament protein CP49 destabilises the lens fibre cell cytoskeleton and decreases lens optical quality, but does not induce cataract. Exp Eye Res 2003; 76:385-91. [PMID: 12573667].

17. Ondruska O, Hanson DM. Raman spectra of duck, rat, and flounder lenses and the formation of dry and cold cataracts. Exp Eye Res 1983; 37:139-43. [PMID: 6617781].

18. Brunkener M, Georgatos SD. Membrane-binding properties of filensin, a cytoskeletal protein of the lens fiber cells. J Cell Sci 1992; 103:709-18. [PMID: 1478967].

19. Rose KM, Wang Z, Magrath GN, Hazard ES, Hildebrandt JD, Schey KL. Aquaporin 0-calmodulin interaction and the effect of aquaporin 0 phosphorylation. Biochemistry 2008; 47:339-47. [PMID: 18081321].

20. Sindhu Kumari S, Gupta N, Shiels A, FitzGerald PG, Menon AG, Mathias RT, Varadaraj K. Role of Aquaporin 0 in lens biomechanics. Biochem Biophys Res Commun 2015; 462:339-45. [PMID: 25960294].

21. Yoon KH, FitzGerald PG. Periplakin interactions with lens intermediate and beaded filaments. Invest Ophthalmol Vis Sci 2009; 50:1283-9. [PMID: 19029034].

22. Blankenship TN, Hess JF, FitzGerald PG. Development- and differentiation-dependent reorganization of intermediate filaments in fiber cells. Invest Ophthalmol Vis Sci 2001; 42:735-42. [PMID: 11222535].

23. Wenke JL, McDonald WH, Schey KL. Spatially Directed Proteomics of the Human Lens Outer Cortex Reveals an Intermediate Filament Switch Associated With the Remodeling Zone. Invest Ophthalmol Vis Sci 2016; 57:4108-14. [PMID: 27537260].

24. Herrmann H, Aebi U. Intermediate filament assembly: temperature sensitivity and polymorphism. Cell Mol Life Sci 1999; 55:1416-31. [PMID: 10518990].

25. Herrmann H, Eckelt A, Brettel M, Grund C, Franke WW. Temperature-sensitive intermediate filament assembly. Alternative structures of Xenopus laevis vimentin in vitro and in vivo. J Mol Biol 1993; 234:99-113. [PMID: 8230211].

26. Gulik-Krzywicki T, Tardieu A, Delaye M. Spatial reorganization of low-molecular-weight proteins during cold cataract opacification. Biochim Biophys Acta 1984; 800:28-32. [PMID: 6743682].

27. Siezen RJ, Fisch MR, Slingsby C, Benedek GB. Opacification of gamma-crystallin solutions from calf lens in relation to cold cataract formation. Proc Natl Acad Sci USA 1985; 82:1701-5. [PMID: 3856852].

28. Tanaka T, Ishimoto C, Chylack LT Jr. Phase separation of a protein-water mixture in cold cataract in the young rat lens. Science 1977; 197:1010-2. [PMID: 887936].

29. Wang K, Cheng C, Li L, Liu H, Huang Q, Xia CH, Yao K, Sun P, Horwitz J, Gong X. GammaD-crystallin associated protein aggregation and lens fiber cell denucleation. Invest Ophthalmol Vis Sci 2007; 48:3719-28. [PMID: 17652744].

30. Bierma JC, Roskamp KW, Ledray AP, Kiss AJ, Cheng CC, Martin RW. Controlling Liquid-Liquid Phase Separation of Cold-Adapted Crystallin Proteins from the Antarctic Toothfish. J Mol Biol 2018; 430:5151-68. [PMID: 30414964].

Articles are provided courtesy of Emory University and the Zhongshan Ophthalmic Center, Sun Yat-sen University, P.R. China. The print version of this article was created on 23 August 2020. This reflects all typographical corrections and errata to the article through that date. Details of any changes may be found in the online version of the article.